Exergetic analysis of the nCO$_2$PP cycle with particular reference to the exergy destruction of sewage sludge due to gasification

Kamil Stasiak[a], Ivar Ståle Ertesvåg[b], Paweł Ziółkowski[a], and Dariusz Mikielewicz[a]

*[a] Gdańsk University of Technology, Gdańsk, Poland, kamil.stasiak@pg.edu.pl, CA,
pawel.ziolkowski1@pg.edu.pl, dariusz.mikielewicz@pg.edu.pl,
[b] Norwegian University of Science and Technology, Trondheim, Norway,
ivar.s.ertesvag@ntnu.no*

Abstract:

An exergy analysis is carried out on the negative CO$_2$ emission gas power plant (nCO$_2$PP), which integrates the process sections of fuel preparation, power generation and carbon capture. Processes of exergy destruction are studied with particular focus on the process in the gasification unit of the fuel preparation section, where a large amount of exergy is destroyed in various chemical reactions from sewage sludge to producer gas conversion. The largest exergy losses are observed in the wet combustion chamber and in the fuel line with the gasification process and water condensation in the gas scrubber, amounting to 126 kW, 43-45 kW and 56 kW respectively, which corresponds to efficiencies of 62%, 89% and 84% of these units, while the exergy efficiency of the power plant is 29.5%. The integration of the gasification unit with the gas scrubber is investigated, and a heat exchanger combination is considered. Ambient air changes in relative humidity and, due to increasing global greenhouse gas emissions, CO$_2$ concentration are analysed. Insight into the theoretical operation of the power plant through exergy analysis allows energy efficiency to be increased by improving areas of highest exergy destruction. To represent real power plant operation, the analysis is based on an optimised process simulation calculated using the most accurate published equations of state, verified with experimental thermophysical property data from the literature.

Keywords:

Exergy Analysis; Efficiency; Gasification; Sewage Sludge; CO$_2$; Process Simulation; Integration; Power Plant.

1. Introduction

The Negative CO$_2$ emission Gas Power Plant (nCO$_2$PP) shown in Figure 1 is the subject of intensive research in a project dedicated to the disposal of sewage sludge with simultaneous generation of electricity and CO$_2$ capture [1]. The nCO$_2$PP cycle has already been described in several articles [2–4] as it offers the hope of simultaneously disposing of the harmful products of human activity (e.g., sewage sludge), then allowing the production of useful electricity, and finally allowing the capture of carbon dioxide in a dedicated part of the CCS. A contribution to the field was made in [5], where an exergy analysis of the nCO$_2$PP system was conducted, investigating aspects of energy efficiency and CO$_2$ capture. The basic equipment includes: (1) the working medium generator - i.e., the wet combustion chamber (WCC), the steam-gas expander (GT+GT^{bap}), the spray-ejector condenser (SEC), and the gasifier in which the sewage sludge is converted into syngas by means of a converter, which is a bleed stream (Fig.1.). Additional equipment includes oxygen, fuel and CO$_2$ compressors, water pumps and heat exchangers. It is extremely important not only to test the syngas production experimentally, but also to model the gasification process correctly to indicate its contribution to the energy conversion chain.

The nCO$_2$PP cycle is consistent with the idea of a bioenergy with a carbon capture and storage (BECCS) power cycle. This involves using a renewable energy source in the form of biomass in combustion processes and then capturing the carbon dioxide produced in this way, ultimately achieving negative CO$_2$ emissions. However, in addition to carbon performance, an important parameter for the sustainable conversion of fuel energy is exergy destruction. One of the critical parameters influencing exergy destruction are ambient parameters such as temperature, humidity and pressure, which have already been classified in many works by some well-known authors on the subject [6,7]. It is worth noting that the effect of CO$_2$ in the air is also beginning to play an increasingly important role in exergy analyses, while the issue of determining the chemical exergy of individual elements still lacks a sufficiently reliable physical basis, and most scholars rely on Szargut

[7] in this area. The situation is even more complicated when determining the chemical exergy of different types of biomass [8]. First of all, there is a lack of a clear chemical and physical foundation to move from well-established methods to determine the composition of the ultimate and proximate type to the exergy, because here, entropy relating to the atomic level plays a role [9]. In the case of the present work, the analyses will focus on a significantly challenging biomass, which is sewage sludge. Attempts to model this process appropriately are being developed particularly intensively in the Aspen Plus environment, where, using mass, momentum and energy balance and the entropy production equation, the exergy destruction due to gasification can be determined [10]. Using these models, it is important to determine the components of the syngas at the reactor outlet and the input supplied to the gasifier. Due to the varying composition of sewage sludge, depending on the region of the world, the calorific value of the sludge and thus, the exergy that is stored in it, also changes [11]. In addition, there is great hope in the production of alternative fuels using sewage sludge, where exergetic analyses supplement information on the quality of energy conversion to useful products such as hydrogen [12] or methanol [13]. With respect to exergetic efficiency, it is possible to provide feedback about sustainable energy conversion. This is because it is necessary to identify possible ways of reducing the destruction of exergy, especially in devices where an alternative solution can be proposed.

In the case of the oxyfuel cycle, which is the subject of this study, it is also important to determine the impact of exergy destruction in separation processes either in an air separation unit (ASU) and a spray-injection condenser (SEC). Industrial ASUs rely on cryogenic methods in order to be able to supply the required amount of oxygen, and methods to reduce power consumption are also found in this part of the system [14]. Thus, exergetic analyses undoubtedly provide an opportunity to study technical and environmental aspects related to energy systems [15]. Therefore, this approach was chosen to analyse the nCO_2 cycle integrated with syngas production in the sludge gasification process.
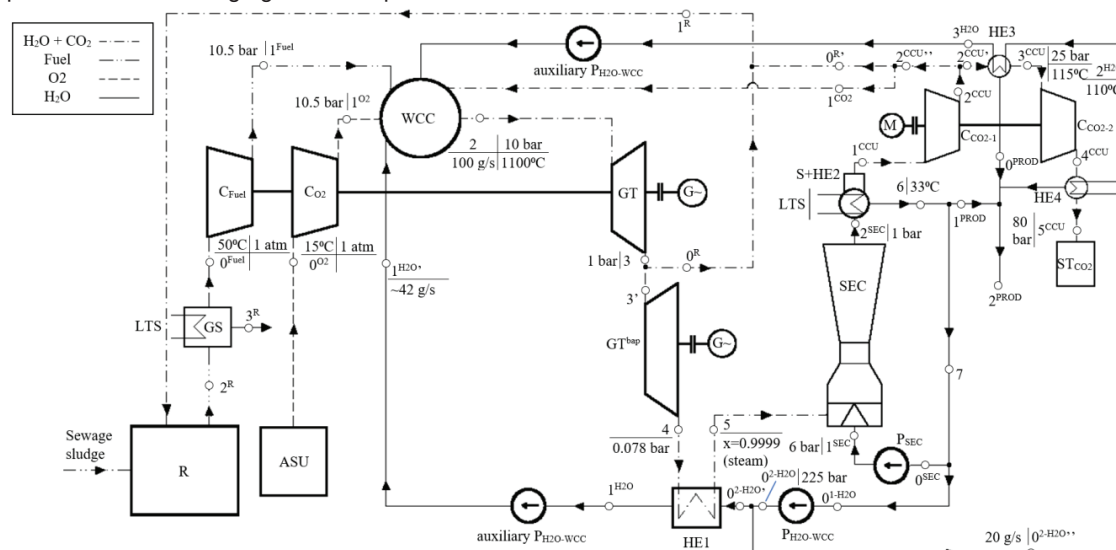

Figure. 1. nCO_2PP process flow diagram [16] where main devices are: WCC – wet combustion chamber, GT – gas turbine, GT^{bap} – low-pressure turbine, R – gasifier, SEC – spray-ejector condenser. Additional devices includes: C_{O2} – oxygen compressor, C_{fuel} – fuel compressor, HE1 – heat exchanger 1, G – generator, $P_{H2O-WCC}$ – WCC water pump, P_{SEC} – SEC pump, S+HE2 – separator connected with heat exchanger 2, C_{CO2-1} and C_{CO2-2} – CO_2 compressors, HE3 – heat exchanger 3, HE4 – heat exchanger 4, GS – gas scrubber, ASU – air separation unit, LTS – lower temperature source.

2. Methodology

2.1. Principal equations

The flow exergy is usually split into a thermomechanical part and a chemical exergy. The latter consists of a mixing part and the chemical exergy component.

$$E^{tot} = E^{th} + E^{ch} \tag{1}$$

The chemical exergy of sewage sludge was calculated as [13]

$$E_{ss}^{ch} = \dot{m}_{ss} \cdot LHV_{ss} \frac{1.0412 + 0.2160 \cdot \left(\frac{H}{C}\right) - 0.2499 \cdot \left(\frac{O}{C}\right) \cdot \left[1 + 0.7884 \cdot \left(\frac{H}{C}\right)\right] + 0.0450 \cdot \left(\frac{N}{C}\right)}{1 - 0.3035 \cdot \left(\frac{O}{C}\right)} \tag{2}$$

The power plant was simulated using Aspen Plus with REFPROP equations of state. A part of the exergy was derived from this software. However, due to the lack of proper documentation of exergy in Aspen software, it was investigated whether this was total exergy, thermomechanical exergy or some part of it. Essentially, total flow exergy is the reversible work done when a flow is brought into equilibrium with its environment. The "Aspen exergy" is the reversible work done when the flow is brought from the relevant state to the Aspen dead state. Due to condensation and phase separation when the flow contains H_2O, the mixture is partially separated. This means that the Aspen exergy calculation includes part of the mixing exergy together with the thermomechanical component. The remaining flow exergy is the reversible work obtained when the flow is brought from the Aspen Plus restricted dead state to equilibrium with the environment:

$$W_{\text{rev}} = T_0 \cdot \bar{R} \cdot \left[\sum_{i \neq H_2O} n_i \cdot ln \frac{n_i}{n - n_{H_2O(liq0)}} + \left(n_{H_2O(g0)} + n_{H_2O(liq0)} \right) \cdot ln \frac{p_{s0: H_2O}(T_0)}{p_0} \right] + n_{H_2O(liq0)} \cdot (p_0 - p_{s0}) \cdot$$

$$\bar{v}_{f: H_2O}(T_0) + \sum_i n_i \cdot \bar{e}_i^{ch} \tag{3}$$

For streams consisting only of liquid water, the equation reduces to the chemical exergy:

$$W_{\text{rev}} = n_{H_2O(liq0)} \cdot \bar{e}_{H_2O(liq0)}^{ch} \tag{4}$$

Including the exergy part calculated by Aspen Plus, the total exergy is as follows:

$$E^{\text{tot}} = E^{\text{Aspen}} + W_{\text{rev}} \tag{5}$$

For the purposes of analysis, exergy destruction was obtained from the steady-state exergy balance,

$$E_d = \sum E_{in}^{\text{tot}} - \sum E_{out}^{\text{tot}} + \sum W_{in} - \sum W_{out} \tag{6}$$

The exergy efficiency of a unit is expressed as the outflow-to-inflow ratio of exergy rates,

$$\eta_{ex} = \frac{\sum E_{out}^{\text{tot}} + \sum W_{out}}{\sum E_{in}^{\text{tot}} + \sum W_{in}} \tag{7}$$

A benefit of the outflow-to-inflow efficiency (compared to the "task efficiency") is that the efficiency of two or more combined units (subsystems) is simply the product of the efficiencies of the individual units. The exergy efficiency of the power plant is then expressed as

$$\eta_{ex|nCO_2PP} = \frac{\sum W_{out} - \sum W_{in}}{E_{fuel,in} + E_{O2,in}} \tag{8}$$

Here, to appreciate the CO_2 capture, the thermodynamic value (pressure and chemical exergy) of the captured CO_2 could be added in the denominator.

2.2. Input data

For exergy analysis, the Aspen Plus dead state was set to the T_0 temperature of 15ºC and p_0 pressure of 1 atm (at sea level 0), which corresponds to most standards. Thus, read values from Aspen Plus with REFPROP equations of state, such as saturation pressure $p_{s0: H_2O}(T_0)$ was 0.0170579 bar and $\bar{v}_{f: H_2O}(T_0)$ was 0.018031 m³/kmol. The exergy calculation also uses the universal gas constant $\bar{R}$ equal to 8.31433 kJ/(kmol K). The chemical exergy calculations used the composition of dry air [17] based on the US Standard Atmosphere, with the CO_2 concentration assumed to be 375 ppm [6] for the year 2004. For comparison, a global average of 417 ppm was used for the year 2022 [18] and a worst-case scenario of 1000 ppm was predicted for the year 2100 [19].
The composition of sewage sludge digested in the gasification unit and fueling the whole power plant, was assumed as mass fractions 27.9% C, 6.7% H, 28.9% O, 4.4% N, 32.2% Ash, with an LHV of 9.8 MJ/kg. The synthesis gas produced by gasification in a steam atmosphere at 760 °C and, after cleaning in the gas scrubber, a volumetric composition of 9.3% CO, 46.8% H_2, 13.9% CH_4, 26.4% CO_2 and 3.5% C_3H_8.

Table 1. Assumptions for the thermodynamic cycle

Parameter	Symbol	Unit	Value
Temperature exhaust after WCC (before GT)	t_2	ºC	1100
Mass flow of the exhaust gas from the WCC	$\dot{m}_2$	g/s	100
Exhaust pressure after WCC	p_2	bar	10
Oxygen-fuel excess ratio in WCC	λ	-	1
Initial syngas temperature, after gas scrubber	t_{fuel}	ºC	50
Initial oxygen temperature	t_{O2}	ºC	15

224

Syngas fuel pressure before C_{fuel} compressor	p_{0-fuel}	bar	1
Oxygen pressure before C_{O2} compressor	p_{0-O2}	bar	1
Fuel to WCC pressure loss factor	δ_{fuel}	-	0.05
Oxygen to WCC pressure loss factor	δ_{O2}	-	0.05
Regenerative water pressure to WCC	p_{1-H2O}	bar	225
Exhaust vapor quality after HE1	x_5	-	0.999
Exhaust temperature after HE1, before SEC	t_5	ºC	33
CO_2 pressure after compressor C_{CCU1}	p_{2-CCU}	bar	25
CO_2 pressure after compressor C_{CCU2}	p_{4-CCU}	bar	80
H_2O temperature after HE4	t_{2-H_2O}	ºC	110
CO_2 temperature after HE3	t_{3-CCU}	ºC	115
Water vapor from Separator in 1^{CCU} mixed with CO_2 vapor	-	%	100% humid
Pressure after GT^{bap}	p_4	bar	0.078
Temperature after SEC	t_6	ºC	35
Turbine GT, internal efficiency (η_i)	η_{iGT}	-	0.89
Turbine GT^{bap}, η_i	$\eta_{iGT-bap}$	-	0.89
Fuel compressor C_{fuel}, η_i	$\eta_{iC-fuel}$	-	0.87
Oxygen compressor C_{O2}, η_i	η_{iC-O2}	-	0.87
WCC water pump $P_{H2O-WCC}$, η_i	$\eta_{iP-H2O-WCC}$	-	0.8
SEC water pump P_{SEC}, η_i	η_{iP-SEC}	-	0.8
CO_2 compressor C_{CO2-1}, η_i	$\eta_{iC-CO2-1}$	-	0.87
CO_2 compressor C_{CO2-2}, η_i	$\eta_{iC-CO2-2}$	-	0.87
Mechanical efficiency for all devices	η_m	-	0.99

3. Results and discussion

Table 2. Calculated chemical components exergy in changing air relative humidity or CO_2 concentration according to [6] and based on Szargut model [7].

Parameter	Symbol	Unit	Value				
Relative Humidity	RH	%	40	50	60	50	50
Atmospheric CO_2 concentration	X_{aCO_2}	ppm	375	375	375	417	1000
Chemical exergies of substances	$\bar{e}^{ch}_{O_2}$	kJ/kmol	3762	3766	3770	3766	3766
	$\bar{e}^{ch}_{CO_2}$	kJ/kmol	18915	18920	18924	18665	16570
	$\bar{e}^{ch}_{H_2O(liq0)}$	kJ/kmol	2195	1661	1224	1661	1661
	$\bar{e}^{ch}_{H_2O(g0)}$	kJ/kmol	11980	11446	11009	11446	11446
	$\bar{e}^{ch}_{H_2}$	kJ/kmol	239121	238585	238146	238585	238585
	$\bar{e}^{ch}_{CO}$	kJ/kmol	275120	275122	275124	274868	272772
	$\bar{e}^{ch}_{CH_4}$	kJ/kmol	836442	835368	834491	835114	833019
	$\bar{e}^{ch}_{C_3H_8}$	kJ/kmol	2157893	2155747	2153991	2154984	2148697

To complete the exergy analysis, the next step was to calculate the chemical exergy of the sludge and calculate the total exergy and efficiency by substituting the chemical exergies from Table 2 above, with the Aspen Plus exergy known from the models. Relative humidities of 40%, 50% and 60% were used for the chemical exergy calculations. For comparison, the changing atmospheric CO_2 concentration of 417 ppm for the global near-surface average in 2022 and the worst-case scenario of 1000 ppm predicted for 2100 were added.

The following tables (Tables 3-13) show the change in exergy rates as a function of the change in dead state parameters. Note that the parameters in Table 1 do not change.

For the gasification unit shown in Table 3, the syngas composition results came from the experiment presented in the authors' other work [2]. Some simplifications were applied: neglecting the exergy of moisture, ash, nitrogen and sulphur, focusing only on the most important aspect from the power generation point of view. A special attention to this process was due to the high water content in the producer gas and its subsequent treatment in a gas scrubber, the exergy analysis of which is shown in Table 4. While applying the simplifications mentioned above, the gas scrubber is simply a condenser in this case. While the producer gas has a high temperature, the waste heat can be recovered during the condensation process, which was not foreseen in the nCO_2PP concept, as the power plant efficiency of BECCS was usually calculated in the literature without

the gasification unit and gas scrubber and overlooked, thus opening a way to increase the overall energy efficiency of the power plant. The exergy efficiency of the gasification unit decreases with higher humidity or CO_2 concentration, and the same is true for the gas scrubber. The exergy destruction had among the largest exergy destruction rates after the WCC, amounting to 43-45 kW and 56 kW for the gasification unit and the gas scrubber, respectively. The exergy efficiency of the gasification unit was close to 89%, while that of the gas scrubber was 84%. The latter can be increased together with the exergy efficiency of the power plant by using water condensation waste heat for the power plant processes.

The following points show the exergy rates as a function of the relative humidity and as a function of the CO_2 content in the air. As can be seen from Tables 5 and 6, the variation of the above parameters did not affect the compressors. In the whole range of the analyzed parameters, the O_2 compressor exergy destruction remained at the level of 0.45 kW, giving an exergy efficiency of 94.6%, while for the fuel compressor the exergy destruction was 0.67 kW and the exergy efficiency 99.8%. It is worth noting that the influence of the environment on the operation of the compressors was reduced to a negligible level due to the lowest exergy rates. Table 7 applies to water pumps, where the effect of the dead state was much more significant. Despite the constant value of exergy destruction, there is a decrease in exergy efficiency with increasing relative humidity. This is related to the change in the value of the exergy rates carried in the water pumped by the pumps. In contrast, a "task efficiency" would give identical results, independent of atmospheric composition.

Heat exchanger 1 (HE 1) results are given in Table 8, with a heat load of 48.6 kW. In this case, the changes in exergy flux were not only for water, but also for the mixture of water vapour and CO_2. A mixture flowed on one side of the exchanger, so the exergy efficiency decreased as both the relative humidity and the proportion of CO_2 in the dead state increase. Also here, a "task efficiency" would be independent of the atmospheric composition.

Table 9, which refers to the water-injected oxy-fuel combustor, is of particular interest as it has several functions in this power plant. Apart from producing working medium with desired parameters for gas turbines, it has oxy-combustion destined for CCU unit, also it reuses water collecting waste heat from other parts of the power plant and cools down the oxy-combustion flame to desired temperature. Hence, it is called a 'wet' combustor. The combustion was assumed stoichiometric with perfect mixing of oxygen and fuel. In reality, some dissociation and kinetics (non-completed reactions) will give a somewhat lower adiabatic flame temperature. The exergy destruction rate of this unit was the largest in the whole power plant yielding about 126 kW, and its exergy efficiency was about 62%, indicating that special attention needs to be paid to improving this process. In relation to the exergy of the sewage sludge fed to the system, this exergy efficiency was 50% when taking into account the whole process from gasification through water condensation in the gas scrubber, compression and mixing effects in the WCC before ignition and after flame generation. It is worth noting that while oxygen mixing with fuel did not cause significant exergy destruction, water mixing into the flame exhaust caused the largest exergy drop in the range of 64-67 kW. Therefore, to increase efficiency, solutions should be sought in the area of water injection to the WCC.

Tables 10 and 11 refer to the main useful energy generator, the high pressure (GT) and low pressure (GT^{bap}) expander with output power of 90.4 kW and 65.7 kW, respectively. The total exergy rates depended slightly on the amount of CO_2 and relative humidity of the atmosphere at dead state. Increasing these parameters gave insignificant changes and virtually no effects on the exergy destruction rates, which were 4.7 kW and 4.8 kW, respectively. In addition, as expected, the gas turbine expanders were characterized by high exergy efficiencies of 97.9% (GT) and 95.6% (GT^{bap}), respectively, at RH=0.4 and 375 ppm CO_2.

Despite significant exergy rates flowing into the SEC, the exergy destruction within this device was negligible. The value of the exergy efficiency, as shown in Table 12, varied from 99.5% to 99.7% in inverse proportion to the increase in relative humidity. It can also be seen that the increase of CO_2 to 1000 ppm in the dead state did not affect the exergy efficiency.

One of the main objectives of the nCO2PP cycle is to capture carbon dioxide. Therefore an indispensable part is to determine the exergy conversion in the Carbon Capture Unit (CCU) island, where the following should be distinguished: heat exchangers HE3 and HE4 (heat duty 12.3 kW), compressors C_{CO2-1} and C_{CO2-2} (power consumption 10.1 kW). The results of the analysis of the exergy destruction rates and the exergy efficiency are presented in Table 13. It can be noted that for the CCU island, there was a clear effect of the amount of CO_2 in the dead state on the exergy efficiency, which decreased from 74.8% for 375 ppm CO_2 (RH=0.5) to 73.2% for 1000 ppm CO_2. This is due to the definition of the efficiency, as the inflow and outflow exergies both decrease with the chemical exergy when increasing atmospheric CO_2. A task efficiency (changed exergy rate by input power) would be unaltered.

226

3.1. Fuel supply line with gasification process

Table 3. Gasifying unit (R).

Function	Medium	t, °C	p, bar	ṁ, g/s	RH, %	40	50	60	50	50
					X_{aCO_2}, ppm	375	375	375	417	1000
					E^{tot}, kW					
Inlet	Sewage Sludge	15	1.013	33.2		375.7	375.7	375.7	375.7	375.7
Inlet	H_2O(g)	100	1.013	27.1		18.0	17.3	16.6	17.3	17.3
Outlet	H_2O(g), CO, CO_2, CH_4, C_3H_8, H_2, without ash	760	1.013	49.6		350.6	349.1	347.9	349.0	347.9
	E_d, kW					43.1	43.8	44.4	43.9	45.0
	η_{ex}, %					89.1	88.9	88.7	88.8	88.5

Table 4. Heat exchanger of Gas Scrubber (GS), Heat Duty = 112.1 kW.

Function	Medium	t, °C	p, bar	ṁ, g/s	RH, %	40	50	60	50	50
					X_{aCO_2}, ppm	375	375	375	417	1000
					E^{tot}, kW					
Inlet	H_2O(g), CO, CO_2, CH_4, C_3H_8, H_2	760	1.013	49.6		350.6	349.4	347.9	349.0	347.9
Outlet	CO, CO_2, CH_4, C_3H_8, H_2	50	1.013	16.6		289.8	289.4	289.1	289.3	288.2
Outlet	H_2O(liq)	50	1.013	33.0		4.7	3.7	2.8	3.7	3.7
	E_d, kW					56.1	56.1	56.1	56.1	56.1
	η_{ex}, %					84.0	83.9	83.9	83.9	83.9

Table 5. Fuel Compressor (C_{fuel}), Work = 8.5 kW.

Function	Medium	t, °C	p, bar	ṁ, g/s	RH, %	40	50	60	50	50
					X_{aCO_2}, ppm	375	375	375	417	1000
					E^{tot}, kW					
Inlet	CO, CO_2, CH_4, C_3H_8, H_2	15	1.013	16.6		289.8	289.4	289.1	289.3	288.2
Outlet	CO, CO_2, CH_4, C_3H_8, H_2	306	10.5	16.6		297.7	297.2	296.9	297.1	296.0
	E_d, kW					0.7	0.7	0.7	0.7	0.7
	η_{ex}, %					99.8	99.8	99.8	99.8	99.8

3.2. Oxygen supply line

Table 6. Oxygen Compressor (C_{O_2}), Work = 5.9 kW.

Function	Medium	t, °C	p, bar	ṁ, g/s	RH, %	40	50	60	50	50
					X_{aCO_2}, ppm	375	375	375	417	1000
					E^{tot}, kW					
Inlet	O_2	15	1.013	20.6		2.4	2.4	2.4	2.4	2.4
Outlet	O_2	313	10.5	20.6		7.9	7.9	7.9	7.9	7.9
	E_d, kW					0.5	0.5	0.5	0.5	0.5
	η_{ex}, %					94.6	94.6	94.6	94.6	94.6

3.3. Water to Wet Combustion Chamber supply line with heat recovery

Table 7. WCC pump ($P_{H2O-WCC}$), Work = 1.8 kW.

Function	Medium	t, °C	p, bar	$\dot{m}$, g/s	RH, % X_aCO2, ppm → E^{tot}, kW	40 / 375	50 / 375	60 / 375	50 / 417	50 / 1000
Inlet	H_2O(liq)	33	1	62.9		2.4	2.4	4.4	5.9	5.9
Outlet	H_2O(liq)	35	225	62.9		9.2	7.4	5.8	7.4	7.4
E_d, kW						0.4	0.4	0.4	0.4	0.4
η_{ex}, %						96.2	95.2	94.1	95.2	95.2

Table 8. Heat Exchanger (HE1), Heat Duty = 48.6 kW

Function	Medium	t, °C	p, bar	$\dot{m}$, g/s	RH, % X_aCO2, ppm → E^{tot}, kW	40 / 375	50 / 375	60 / 375	50 / 417	50 / 1000
Inlet	H_2O(liq)	35	225	42.9		6.3	5.0	4.0	5.0	5.0
Outlet	H_2O(liq)	294	225	42.9		22.2	20.9	19.9	20.9	20.9
Inlet (exhaust)	H_2O(g), CO_2	323	0.078	100		41.9	39.7	37.8	39.5	38.4
Outlet (exhaust)	H_2O(g), CO_2	40	0.078	100		25.0	22.8	20.9	22.6	21.5
E_d, kW						1.0	1.0	1.0	1.0	1.0
η_{ex}, %						98.0	97.8	97.6	97.8	97.7

3.4. Wet Combustion Chamber and expansion

Table 9. Wet Combustion Chamber (WCC) with chemical energy rate according to LHV = 282 kW, and according to HHV = 317 kW

Function	Medium	t, °C	p, bar	$\dot{m}$, g/s	RH, % X_aCO2, ppm → E^{tot}, kW	40 / 375	50 / 375	60 / 375	50 / 417	50 / 1000
Inlet (syngas)	CO, CO_2, CH_4, C_3H_8, H_2	306	10.5	16.6		297.7	297.2	296.9	297.1	296.0
Inlet	O_2	313	10.5	20.6		7.9	7.9	7.9	7.9	7.9
Inlet	H_2O(liq)	181	225	20		5.8	5.2	4.7	5.2	5.2
Inlet	H_2O(liq)	294	225	42.9		22.2	20.9	19.9	20.9	20.9
Intermediary	O_2 (mixing with:), CO, CO_2, CH_4, C_3H_8, H_2	308	10.5	37.2		303.0	302.6	302.3	302.5	301.4
Flame	H_2O(g), CO_2	4260	10	37.2		271.1	270.7	270.4	270.6	269.5
Outlet	H_2O(g), CO_2	1100	10	100		207.3	205.0	203.1	204.9	203.7
E_d, kW						126.3	126.3	126.3	126.3	126.3
η_{ex}, %						62.1	61.9	61.7	61.9	61.7

Table 10. Gas Turbine (GT), Work = 90.4 kW

Function	Medium	t, °C	p, bar	ṁ, g/s			E^{tot}, kW		
	RH, %				40	50	60	50	50
	X_{aCO_2}, ppm				375	375	375	417	1000
Inlet	H_2O(g), CO_2	1100	10	100	207.3	205.0	203.1	204.9	203.7
Outlet	H_2O(g), CO_2	672	1	100	112.5	110.2	108.3	110.0	108.9
E_d, kW					4.7	4.7	4.7	4.7	4.7
η_{ex}, %					97.9	97.8	97.8	97.8	97.8

Table 11. Gas Turbine below ambient pressure (GT^{bap}), Work = 65.7 kW

Function	Medium	t, °C	p, bar	ṁ, g/s			E^{tot}, kW		
	RH, %				40	50	60	50	50
	X_{aCO_2}, ppm				375	375	375	417	1000
Inlet	H_2O(g), CO_2	672	1	100	112.5	110.2	108.3	110.0	108.9
Outlet	H_2O(g), CO_2	323	0.078	100	41.9	39.7	37.8	39.5	38.4
E_d, kW					4.8	4.8	4.8	4.8	4.8
η_{ex}, %					95.7	95.6	95.6	95.6	95.6

3.5. Ending of the expansion with CO₂ processing

Table 12. Spray Ejector Condenser (SEC) with Separator, Pump Work = 18.2 kW

Function	Medium	t, °C	p, bar	ṁ, g/s			E^{tot}, kW		
	RH, %				40	50	60	50	50
	X_{aCO_2}, ppm				375	375	375	417	1000
Inlet (motive fluid)	H_2O(liq)	33	1	28740	3564.3	2712.1	2015.8	2712.1	2712.1
Inlet (exhaust)	H_2O(g), CO_2	40	0.078	100	25.0	22.8	20.9	22.6	21.5
Outlet	H_2O(g)+CO_2	35	1	23.7	10.0	10.0	10.0	9.8	8.7
Outlet	H_2O(liq)	35	1	28816	3586.2	2731.8	2033.6	2731.8	2731.8
E_d, kW					11.3	11.3	11.3	11.3	11.3
η_{ex}, %					99.7	99.6	99.5	99.6	99.6

Table 13. Carbon Capture Unit (CCU), HE3 and HE4 cooling heat duty = 12.3 kW, compressors C_{CO2-1} and C_{CO2-2} Work = 10.1 kW

Function	Medium	t, °C	p, bar	ṁ, g/s			E^{tot}, kW		
	RH, %				40	50	60	50	50
	X_{aCO_2}, ppm				375	375	375	417	1000
Inlet	H_2O(g)+CO_2	35	1	23.7	10.0	10.0	10.0	9.8	8.7
Outlet	H_2O(liq)	65	80	0.5	0.07	0.06	0.04	0.06	0.06
Outlet	H_2O(g)+CO_2	65	80	23.2	15.0	15.0	15.0	14.8	13.7
E_d, kW					7.4	7.4	7.3	7.4	7.4
η_{ex}, %					74.8	74.8	74.8	74.6	73.2

3.6. nCO₂PP exergy efficiency

While the cumulative efficiency of the power plant in the studied combination is 27.88% [16], its exergy efficiency according to Eq. (8) is 29.48% when related to the exergy of the sewage sludge used as input and is constant for varying RH or CO_2 concentration, although the value starts to vary when related to the producer gas.
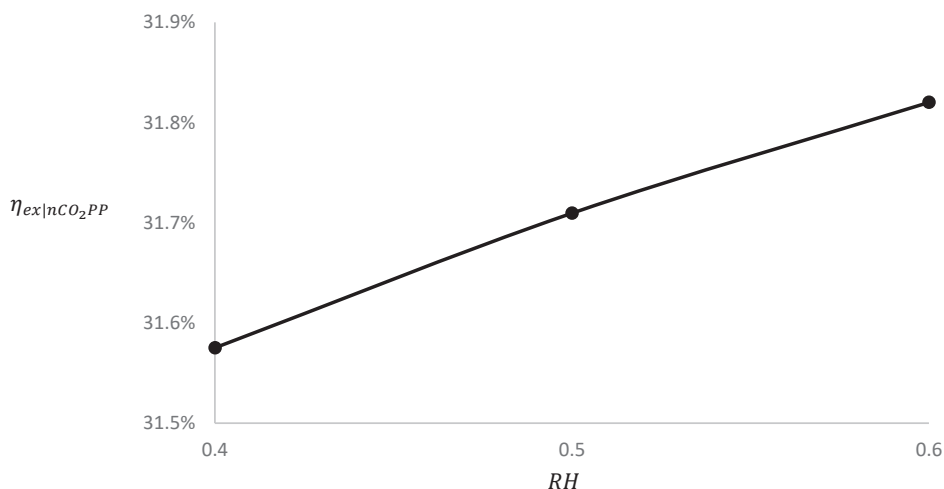

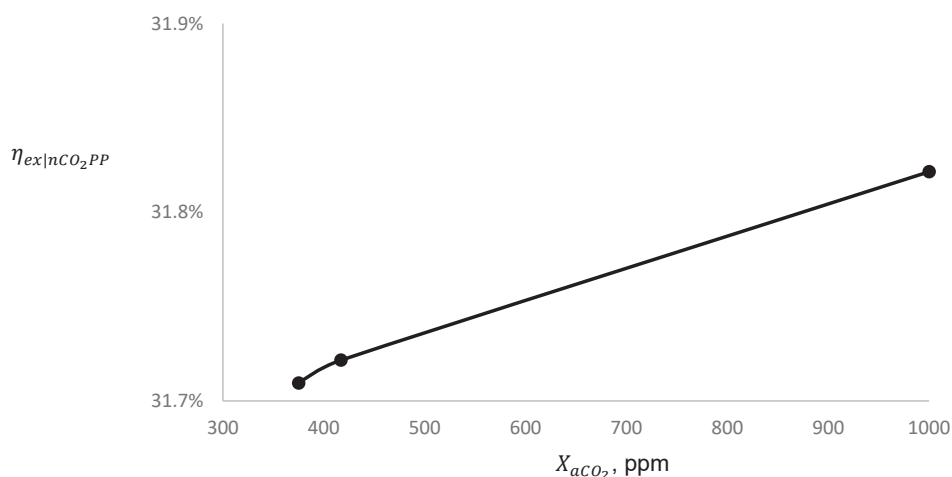**Figure. 2.** nCO₂PP exergy efficiency in changing air humidity conditions

Figure. 3. nCO₂PP exergy efficiency in changing air CO_2 concentrations

4. Conclusions

Second law analysis has been conducted on nCO₂PP. The analyses gave an insight into the integrated system of the gasifier and the nCO₂PP cycle, taking into account the influence of relative humidity and CO_2 content in the air, which translated into chemical exergy of the components in relation to the dead state. The conducted analyses showed that the lowest exergy efficiency is characterized by a wet combustion chamber with a value of about 62%. However, exergy losses affecting the efficiency of this device are unavoidable. Another significant loss is the CO_2 conditioning system for later storage with an exergy efficiency value of 75%. Also, in this set of devices, the possibilities of reducing exergy destruction are limited. Another device with a relatively low exergy efficiency is the gasifier unit and the heat exchanger of gas scrubber with efficiencies of 89% and 84%, respectively. Significant prospects for reducing exergy destruction are offered by the Heat exchanger of Gas Scrubber because the waste heat from this device can be used to drive organic Rankine cycles or to produce oxygen in oxygen transport membranes.

Acknowledgments

Nomenclature

E	flow exergy rate, kW
E_d	exergy destruction rate, kW
$\bar{e}$	specific molar exergy, kJ/kmol
$\dot{m}$	mass flow rate, g/s
p	pressure, bar
RH	air relative humidity, %
t	temperature, °C
W	work rate (power), kW

Greek symbols

η	efficiency

Subscripts and superscripts

aCO_2	CO_2 in atmospheric air
$Aspen$	derived from Aspen Plus
ch	chemical
ex	exergetic
$fuel, in$	either sewage sludge or producer gas input to the power plant system
nCO_2PP	negative CO_2 emission gas power plant project
O_2, in	oxygen input to the power plant system
rev	reversible
th	thermomechanical
tot	total

References

[1]   Negative CO2 Emission Gas Power Plant Project site 2023. nco2pp.com (accessed February 26, 2023).

[2]   Ziółkowski P, Badur J, Pawlak- Kruczek H, Stasiak K, Amiri M, Niedzwiecki L, et al. Mathematical modelling of gasification process of sewage sludge in reactor of negative CO2 emission power plant. Energy 2022;244. https://doi.org/10.1016/j.energy.2021.122601.

[3]   Ziółkowski P, Madejski P, Amiri M, Kuś T, Stasiak K, Subramanian N, et al. Thermodynamic analysis of negative CO2 emission power plant using aspen plus, aspen Hysys, and ebsilon software. Energies (Basel) 2021;14. https://doi.org/10.3390/en14196304.

[4]   Stasiak K, Ziółkowski P, Mikielewicz D. Carbon Dioxide Recovery Skid. Progress in Petrochemical Science 2020;3:362–4. https://doi.org/10.31031/pps.2020.03.000570.

[5]   Ertesvåg IS, Madejski P, Ziółkowski P, Mikielewicz D. Exergy analysis of a negative CO2 emission gas power plant based on water oxy-combustion of syngas from sewage sludge gasification and CCS. Energy 2023;278:127690. https://doi.org/10.1016/J.ENERGY.2023.127690.

[6]   Ertesvåg IS. Sensitivity of chemical exergy for atmospheric gases and gaseous fuels to variations in ambient conditions. Energy Convers Manag 2007;48:1983–95. https://doi.org/10.1016/J.ENCONMAN.2007.01.005.

[7]   Szargut J. Chemical exergies of the elements. Appl Energy 1989;32:269–86. https://doi.org/10.1016/0306-2619(89)90016-0.

[8]   Aghbashlo M, Tabatabaei M, Nadian MH, Soltanian S, Ghasemkhani H, Shafizadeh A, et al. Determining biomass chemical exergy using a novel hybrid intelligent approach to promote biomass-

https://doi.org/10.52202/069564-0021

based biorefineries. J Clean Prod 2020;277:124089. https://doi.org/10.1016/J.JCLEPRO.2020.124089.

[9] Qian H, Zhu W, Fan S, Liu C, Lu X, Wang Z, et al. Prediction models for chemical exergy of biomass on dry basis from ultimate analysis using available electron concepts. Energy 2017;131:251–8. https://doi.org/10.1016/J.ENERGY.2017.05.037.

[10] Zhang F, Wang S, Li Y, Chen W, Qian L. Thermodynamic analysis of a supercritical water gasification – oxidation combined system for sewage sludge treatment with cool wall reactor. Energy Convers Manag 2021;247:114708. https://doi.org/10.1016/J.ENCONMAN.2021.114708.

[11] Ruya PM, Purwadi R, Lim SS. Supercritical water gasification of sewage sludge for power generation– thermodynamic study on auto-thermal operation using Aspen Plus. Energy Convers Manag 2020;206:112458. https://doi.org/10.1016/J.ENCONMAN.2019.112458.

[12] Abuşoğlu A, Özahi E, Kutlar Aİ, Demir S. Exergy analyses of green hydrogen production methods from biogas-based electricity and sewage sludge. Int J Hydrogen Energy 2017;42:10986–96. https://doi.org/10.1016/J.IJHYDENE.2017.02.144.

[13] Ptasinski KJ, Hamelinck C, Kerkhof PJAM. Exergy analysis of methanol from the sewage sludge process. Energy Convers Manag 2002;43:1445–57. https://doi.org/10.1016/S0196-8904(02)00027-4.

[14] Fu C, Gundersen T. Using exergy analysis to reduce power consumption in air separation units for oxy-combustion processes. Energy 2012;44:60–8. https://doi.org/10.1016/J.ENERGY.2012.01.065.

[15] Szargut J. Exergy method: technical and ecological applications. International Series on Developments in Heat Transfer 2005;18.

[16] Ziółkowski P, Stasiak K, Amiri M, Mikielewicz D. Negative carbon dioxide gas power plant integrated with gasification of sewage sludge. Energy 2023;262:125496. https://doi.org/10.1016/j.energy.2022.125496.

[17] David R. Lide. CRC Handbook of Chemistry and Physics 80th Edition. 1999.

[18] Friedlingstein P, O'Sullivan M, Jones MW, Andrew RM, Gregor L, Hauck J, et al. Global Carbon Budget 2022. Earth Syst Sci Data 2022;14:4811–900. https://doi.org/10.5194/essd-14-4811-2022.

[19] Schneider S. The worst-case scenario. Nature 2009;458:1104–5. https://doi.org/10.1038/4581104a.